Structural Monitoring and Maintenance, *Vol. 2, No. 1 (2015) 1-18*
DOI: http://dx.doi.org/10.12989/smm.2015.2.1.001

Modal parameters identification of heavy-haul railway RC bridges – experience acquired

Regina Sampaio*[1] and Tommy H.T. Chan[2a]

[1]*Faculty of Civil Engineering, Federal University of Pará - UFPA, Belem 66075-110 Brazil*
[2]*Faculty of Science and Engineering, Queensland University of Technology - QUT, Brisbane 4001, Australia*

(Received January 9, 2015, Revised March 3, 2015, Accepted March 5, 2015)

Abstract. Traditionally, it is not easy to carry out tests to identify modal parameters from existing railway bridges because of the testing conditions and complicated nature of civil structures. A six year (2007-2012) research program was conducted to monitor a group of 25 railway bridges. One of the tasks was to devise guidelines for identifying their modal parameters. This paper presents the experience acquired from such identification. The modal analysis of four representative bridges of this group is reported, which include B5, B15, B20 and B58A, crossing the Carajás railway in northern Brazil using three different excitations sources: drop weight, free vibration after train passage, and ambient conditions. To extract the dynamic parameters from the recorded data, Stochastic Subspace Identification and Frequency Domain Decomposition methods were used. Finite-element models were constructed to facilitate the dynamic measurements. The results show good agreement between the measured and computed natural frequencies and mode shapes. The findings provide some guidelines on methods of excitation, record length of time, methods of modal analysis including the use of projected channel and harmonic detection, helping researchers and maintenance teams obtain good dynamic characteristics from measurement data.

Keywords: railway bridges; operational modal analysis; stochastic subspace identification; frequency domain decomposition

1. Introduction

Railway bridges are large and complex structures subjected to dynamic loads and thus need a thorough evaluation to ensure satisfactory use, especially after many years of operation under heavy traffic conditions. Structural health monitoring based on dynamic measurements is a very active field, especially in bridge engineering (Shih *et al.* 2011, Moradipour *et al.* 2015). However, the experimental evaluation of dynamic parameters can be very challenging, particularly in the case of large and heavy structures such as bridges. It may be very difficult and/or inconvenient to excite a structure with a known input force because this procedure usually causes traffic interruption. Thus, a number of papers have been published on output-only modal analysis techniques. In the case of railway bridges, when freight train passages are used to excite the structure, it is clear that the train exerts a great influence on the system modal parameters due to

*Corresponding author, Associate Professor, E-mail: rsampaio@ufpa.br
[a] Professor, E-mail: tommy.chan@qut.edu.au

http://www.techno-press.org/?journal=smm&subpage=7 ISSN: 2288-6605 (Print), 2288-6613 (Online)

strong bridge-vehicle interaction effects (Lee *et al.* 2006).

In this paper, modal analysis of reinforced concrete bridges of a heavy haul single track railway is under investigation. An experimental program was implemented and acceleration data was obtained under operational conditions. Some aspects on the operational modal analysis (OMA) are discussed.

Those reinforced concrete bridges have short to medium spans (9.5 to 25 m) and could be considered as quite rigid, so they are difficult to excite, as noise can be the same level as the structural vibration. Data was obtained for each train passage, for ambient vibration between train passages and for vibration due to people jumping or using a “drop weight” system. From data obtained with train passages only the free vibration part were used to obtain the dynamic characteristics of the bridge.

Using commercial software Artemis® (SVS 2011) to identify the modal parameters, Stochastic Subspace Identification (SSI) techniques and Frequency Domain Decomposition (FDD) technique were used and compared between each other and with results from a computational model.

2. Description of bridge network

The bridges under analysis are part of a bridge network of the Carajás railway. This single track railway of 892 km is mainly used to transport iron ore from Carajás ore mine to Ponta da Madeira port in northern Brazil and has 54 bridges. Except for the bridge over the river Tocantins, which has quite different characteristics, the other 53 bridges have short to medium spans and are classified in 26 groups according to their material type, section, structural system and number of spans. Regarding materials, 44 are reinforced concrete bridges, 7 are prestressed concrete bridges and 2 are prestressed concrete bridges with one steel truss span. The trains that operate on this railway are hauled by three diesel-electric locomotives (with 300 kN per axle) and have 208 freight cars (with 325 kN per axle when loaded, and 52.5 kN per axle when unloaded). The owner of the railway, Vale mining company, intends to increase the loads of the trains and is concerned about the load-carrying capacity of the bridges of the network. Since these bridges are about 30 years old, it prompts the need to assess theactual condition of these railway bridges.

Therefore, Carajás railway was monitored between 2007 and 2012 by a research program conducted by Federal University of Pará in partnership with Vale. In this program, accelerations and strains were collected in 25 railway bridges as representativesfrom groups. Samples were obtained during the passage of loaded and unloaded iron ore trains and other types of trains, like passenger trains. Samples were collected when structure were under ambient vibration and with the use of a drop weight system, as well.

This paper shows the modal analysis of four reinforced concrete bridges of those monitored, Bridges B5, B15, B20; and B58A. These bridges were chosen because they roughly represent 4 different groups of those mentioned above and these 4 groups are formed by 13 bridges of Carajás railway. In addition, the visual inspection of them indicated that they are in a good condition. This paper aims to present all the work involved in the monitoring program for these four bridges and show results of the modal analysis that could lead to a methodology of analysis for all data collected and also share the experience in acquiring dynamic characteristics using vibration tests.

3. Description of bridges

Fig. 1 shows a general view of four bridges. All four bridges analyzed have a straight alignment. Bridges B5, B15 and B20 are formed by continuous spans with cross section and support conditions described in Table 1 and Fig. 2(a). B58A is a simply supported span and its typical cross section is shown in Fig. 2(d).

The reinforced concrete girders rest on elastomeric (neoprene) laminated bearings, disposed on the top of the bents or caisson caps and on the abutment supports.

B20 substructure is formed by single column bents of rectangular box cross-section, fixed at the pile caps, the other bridges rest directly on the foundation blocks. The foundation of those four bridges consists of caissons. The abutments have a hollow rectangular shape, consisting of individual chambers separated by diaphragm walls which are filled with gravel (ballast), and are also supported on foundation blocks.

(a) B5

(b) B15

(c) B20

(d) B58A

Fig. 1 Bridges overview

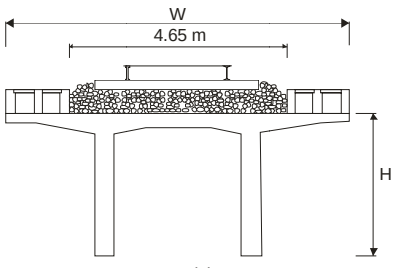

(a) B20, B15 and B5

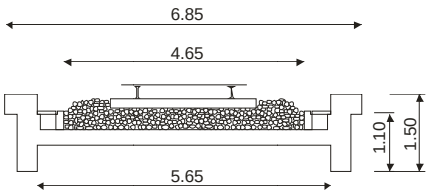

(b) B58A

Fig. 2 Sketch of typical cross sections

Table 1 Geometric characteristics and structural system of the bridges

Bridge	Number of spans	Span (m)	Structural System	Type of material	Section	W*(m)	H*(m)
5	3	18	Continuous span, simply supported at both ends (abutments)	Reinforced Concrete	Pi-shaped girder	6.75	2.40
15	3	20	Continuous span, one end clamped (abutment1) without intermediary joints	Reinforced Concrete	Pi-shaped girder	5.85	2.80
20	5	22.5	Continuous span, one end clamped (abutment2) without intermediary joints	Reinforced Concrete	Pi-shaped girder	5.85	3.00
58A	1	9.5	Simply supported span	Reinforced Concrete	H shaped girder	**	**

*indicated in Fig. 2(a) ** Not applicable, see Fig. 2(b) for details

4. Monitoring program

Bridges under study were monitored with 20 low frequency accelerometers Wilcoxon® 793L (http://www.wilcoxon.com/vi_index.cfm?PD_ID=11) with nominal sensitivity of 500 mV/g (Fig. 4(a)) connected to two Lynx® ADS-2000 data acquisition system, each with 16 channels (Fig. 4(b)). The accelerometers were mounted on metallic base plates attached to the bridge deck with high strength adhesive. The acquisition sample frequency was chosen to be 400 Hz.

4.1 Deployment of sensors

The accelerometers were installed at selected locations (stations) along both sides of bridges decks covering the whole length of the bridges as shown in Fig. 3. Those locations were chosen according with a preliminary finite element model. At B15 and B20, the accelerometers were relocated to different measurement stations, with fixed accelerometers at reference stations as indicated in Fig. 3. Reference stations were used due to the limited number of sensors available and the limitation of the maximum cable length in 50 meters, as the common arrangement for bridge dynamic tests.

It is worth mentioning that in B15, only data obtained from the right side sensors were considered since a considerable number of sensors located at the left side presented a very high noise. For this reason, it was not possible to identify torsion modes for this bridge.

4.2 Excitations

The main difficulty concerning dynamic measurements of civil engineering structures is usually the excitation. In case of bridge operational modal analysis, this is particularly true if the bridge span is short to medium and if it is only used by heavy freight trains.

For the present study, the system modal identification was made using three types of recorded signals. Free vibration records were collected immediately after the passage of loaded trains (FV) with a record length time correspondent to amplitude decay time.

Depending on the railway traffic, ambient vibration tests (AV) were performed. The lengths of data obtained were: 59 min for B15 and 25 min for B58A and B5. Considering the first bending period in vertical and transversal directions for these bridges, the relation between the record length and the natural period of the structure, which is the inverse of the natural frequency, is shown in Table 2.

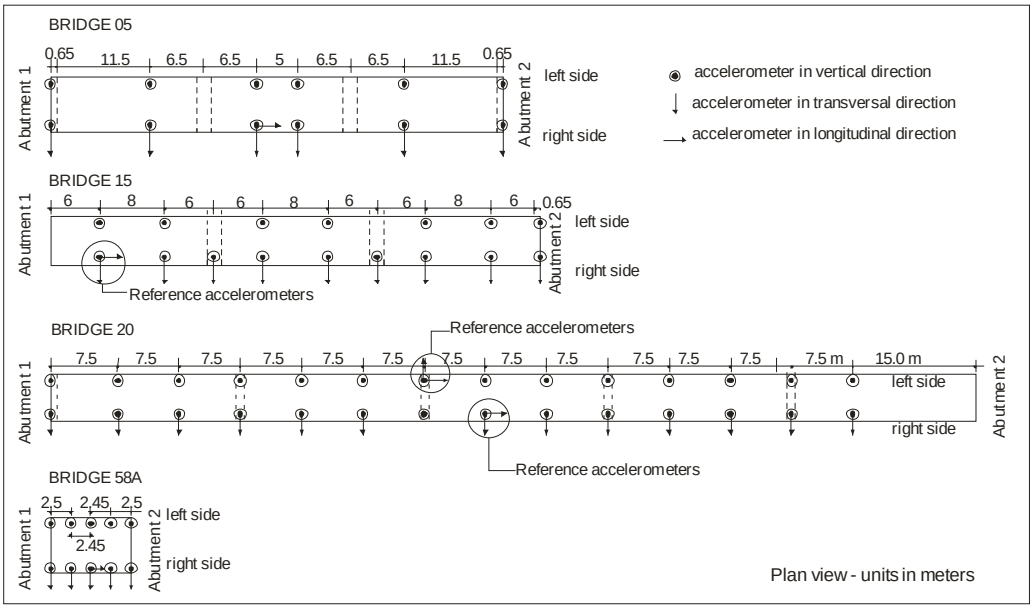

Fig. 3 Accelerometer layout

Table 2 Relation between Record length time and first bending period – Ambient vibration tests

Bridge	Record Length (in min)	Record Length (in s)	1st lateral bending (FEM)		1st vertical bending (FEM)		Recorded time/Lat. period (s/s)	Recorded time/Vert. Period (s/s)
			Freq. (Hz)	Period (s)	Freq. (Hz)	Period (s)		
5	25	1500	4.16	**0.24**	9.24	**0.11**	6.2E+03	1.39E+04
15	59	3540	0.82	**1.22**	5.04	**0.20**	2.9E+03	1.79E+04
58A	25	1500	xx	**xx**	12.66	**0.08**	xx	1.90E+04

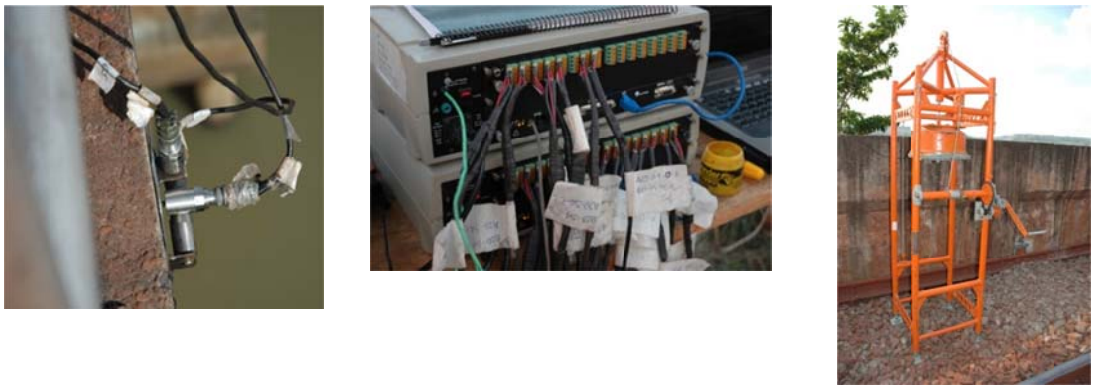

(a) Mounting accelerometers on bridge deck (b) Data acquisition system (c) Drop-weight system

Fig. 4 Monitoring program – Sensors, data acquisition system and drop-weight system

It was not possible to obtain records sufficiently long for B20 because of some issues regarding weather during tests on this bridge and it was not allowed to conduct tests during the night for safety reasons.

After first series of tests on B15, records using other type of excitation, a drop-weight system (DW), were also collected. This consists of a weight of 100 kg released on bridge deck from 1.5 m height, built for this purpose (Fig. 4(c)).

4.3 Modal identification methodology

Two methods were used on purpose to analyse the data: 1) Enhanced Frequency Domain Decomposition technique (EFDD) and 2) Stochastic Subspace Identification technique (SSI). Those techniques are implemented in a commercial software package Artemis® (SVS 2011).

The EFDD is a method that can be understood as an extension of the simply peak picking the peaks of the spectral estimates of the measured signals to identify the Eigen frequencies. It uses the response power spectral densities, but introduces an operation in Power Spectral Density (PSD) matrix, which is decomposed by taking the Single Value Decomposition (SVD) of power spectral density matrix (Brincker 2000 and Brincker *et al*. 2001).

Another methodology, in time domain, used to perform modal extraction was the SSI method. The SSI technique directly works with time data without the need to convert them to correlations or spectra (Ren *et al.* 2005). The SSI algorithm identifies state space matrices based on the measurements using robust numerical techniques such as QR factorization, singular value decomposition (SVD), and least squares. Once the mathematical description of the structure (the state space model) is found, the modal parameters can be determined in a straight forward manner (Ren *et al*. 2005). The theoretical background is given in (Van Overschee and de Moor 1993, Peeters 2000, Ubertini *et al*. 2013)

The analysis was performed considering the use of projection channels. As mentioned by Herlufsen *et al*. (2006), in the case where a large number of sensors are used simultaneously the parametric model fit in SSI analysis suffers from the estimation of many noise modes, compared to

the number of physical modes of the system. The main reason for this is that the many channels contain the same physical information but different random errors (Herlufsen *et al*. 2006). The use of projection channels decreases the amount of redundant information and the estimated models tends to stabilize faster, i.e., at lower state space dimensions (corresponding to "smaller" subspaces). Nguyen *et al*. (2014 a, b) also observed the importance on the use of projection technique in presence of data synchronization error and show that SSI- method failed on detecting some modes and some modes were mistakenly detected as noise if the channel projection is not used.

The choice of the projection channels starts with the channel that correlate most with all the other channels. In case of multiple data sets the user-defined reference channels are applied as initial projection channels.

It is noteworthy that the choice of the number of projection channels must be done carefully. As an example, Fig. 5 shows the Stabilization Diagrams in a frequency range of 5 to 9 Hz, for tests with drop weight in B20, considering: a) without projection channels; b) three projection channels and c) four projection channels.

In this Stabilization diagram, the vertical lines formed by red symbols represent the stable modes identified while the vertical lines formed by brown symbols indicate the noise modes. The green symbols, in turn, are unstable modes. The Stabilization Diagram is plotted over the graph of singular values of the spectral density matrix (SVD plot), whose peaks indicate a possible frequency of the system.

As mentioned early, bridge B20 was monitored with 44 accelerometers measured in 3 data sets. Analysis without the use of projection channels gives unreliable results (the red lines do not match the peaks of the SVD graphic) and the use of 4 projection channels also miss one mode (the red lines do match one peak of the SVD graphic), so the stabilization diagram shows an optimal choice of three projection channels (the red lines match two peaks of the SVD graphic), which was the minimum number stated by Artemis for this case.

The number of projection channels selected for each case was the one that provided the best results, although in most of the cases it was the minimum number stated by Artemis software.

The algorithms used in operational modal analysis assume that the input forces are stochastic in nature. Although, this is often the case for civil engineering structures sometimes rotational forces are seen as harmonic components in the responses, and their influence should be eliminated before extracting the modes in their vicinity. Also, in order to eliminate the influence of the harmonic components in the modal parameter extraction process, the harmonic detection option was enabled in Artemis. As stated by Jacobsen *et al*. (2007), the consequences of having harmonic components from sinusoidal excitations present in the responses depend on both the nature of the harmonic components (number, frequency and level) and the modal parameter extraction method used. For the EFDD technique it is important that harmonic components inside the desired single degree of freedom are identified and their influence eliminated before proceeding with the modal parameter extraction process.

In the present study, the option for checking the presence of harmonics comes from a particular situation; generators and drill machines had been used on the bridges during the tests. However, even though some harmonics have been detected in the frequency range of interest, they do not show much influence in obtaining the structure vibration modes.

In pre-processing, a high-pass filter with frequency of 0.1 Hz and order 2 was used to eliminate excessive noise in the data collected with the drop weight system and ambient vibration. A high-pass filtering of the signals can make the identification of the lower modes, using the SSI

technique, much easier.

Preliminary finite element models were built to allow a preliminary assessment of the structure and thus provide background for choosing both the position of the sensors as the frequency band of interest. So, for B5, B15 and B20, the frequency range of interest lies between 0 and 15 Hz. The sampling frequency on site was chosen to be 400 Hz as mentioned early, and afterwards, the data was resampled at 40 Hz. Since the anti-aliasing filter was active in the frequency range of the decimate signal, the modal results was considered with a cut-off frequency of 80% of the Nyquist frequency, so a cut-off frequency of 16 Hz. The applied antialiasing filter is an 8^{th} order Chebyshev lowpass filter. For B58A, the frequency range of interest is between 0 and 30 Hz, so the decimation factor was chosen for the purpose of obtain a Nyquist frequency of 40 Hz, giving a cut-off frequency of 32 Hz. Other decimation factors were used to magnify the results in a low frequency range, trying to identify low frequency mode shapes associated to lateral bending in B5, B15 and B20.

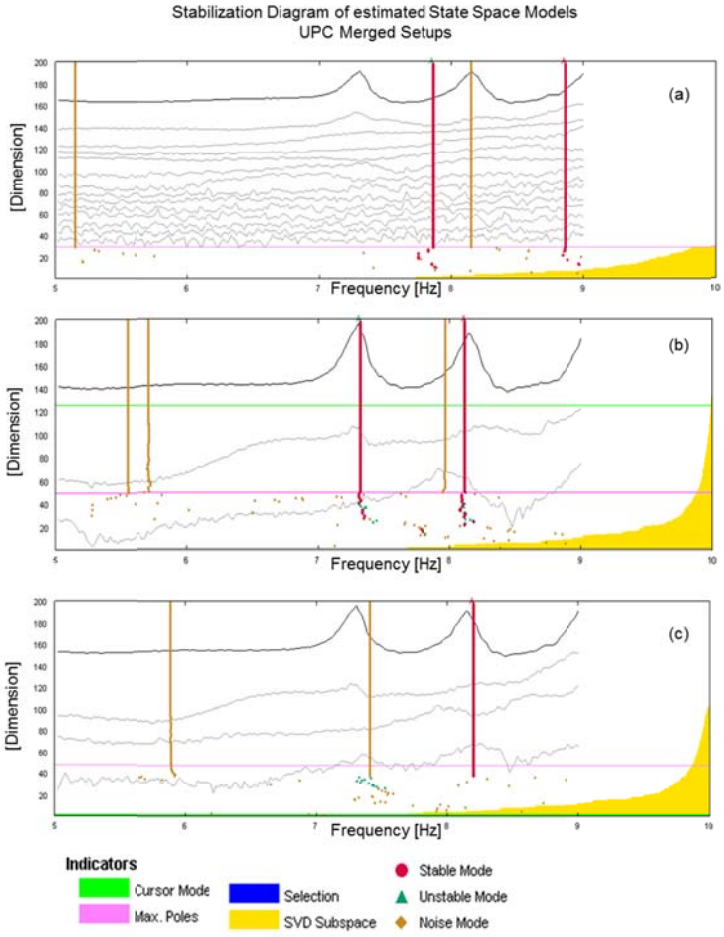

Fig. 5 Stabilization diagram in a frequency range of 5 to 9 Hz, for tests with drop weight in Bridge 20, considering: (a) without projection channels and (b) 3 projection channels and (c) 4 projection channels

5. Modal identification

The results concerning the estimated frequency and damping values obtained from analysis using EFDD and SSI methods and for all types of records are summarized in Table 3 for B5, B15, B20 and B58A. The numerical natural frequencies of updated finite element models are shown in the last column of Table 3.

For B15 and B20, it was possible to identify up to five modes, despite the drop weight system had not been used for Bridge B15 and the ambient vibrations was not possible to be used for B20. For B5, up to four modes were identified. For tests using the Drop Weight system on B5 and B20, it was possible to identify a vertical bending mode that was not identified using Ambient Vibration or Free Vibration and which is in a good agreement with a numerical mode shape as shown in Table 5 for mode 2 of B5 and for mode 4 of B20.

Damping factors, in turn, are always difficult to estimate exactly, and the results presented in Table 3 are very dispersive. The sources for energy dissipation are various and different from the viscous type used in the theoretical formulation of the vibration problems. Particularly the damping due to friction between ballast particles can play an important role in this type of structures.

Table 3 Frequencies and damping factors extracted from experimental modal analysis and numerical frequencies obtained using Finite Element Method (FEM) models

		Free Vibation				Drop Weight				Ambient Vibration					
		SSI		EFDD		SSI		EFDD		SSI		EFDD		Mode	FEM
Bridge	N	**Frq. (Hz)**	Damp.	**Frq. (Hz)**	Damp.	**Frq. (Hz)**	Damp.	**Frq. (Hz)**	Damp.	**Frq. (Hz)**	Damp.	**Frq. (Hz)**	Damp.	Type	Frq. (Hz)
5	1	**8.91**	1.36%	**9.17**	0.24%	**9.03**	0.85%	9.01	0.96%	9.23	1.57%	**9.28**	1.34%	Vertical bending	9.24
	2	xx	xx	xx	xx	**10.84**	1.99%	xx	xx	xx	xx	xx	xx	Vertical bending	10.19
	3	**11.15**	0.17%	**11.13**	0.50%	**12.60**	0.78%	xx	xx	**11.96**	0.45%	**12.04**	0.78%	Vert.&lat .Bending	11.55
	4	**13.06**	0.57%	xx	xx	**13.14**	1.05%	13.12	1.02%	xx	xx	**13.34**	0.86%	torsion	xx
15	1	xx	xx	xx	xx	xx	xx	xx	xx	**2.46**	3.70%	**2.45**	1.09%	lateral bending	2.41
	2	**7.46**	1.96%	xx	xx	xx	xx	xx	xx	**7.47**	0.52%	**7.46**	0.65%	Vertical bending	7.92
	3	**8.53**	2.15%	xx	xx	xx	xx	xx	xx	xx	xx	xx	xx	lateral bending	8.78
	4	xx	xx	xx	xx	xx	xx	xx	xx	**10.40**	1.18%	xx	xx	Vertical bending	9.11
	5	**11.20**	0.85%	xx	xx	xx	xx	xx	xx	**11.15**	1.49%	**11.23**	1.72%	Vertical bending	11.68
20	1	**2.58**	2.29%	xx	xx	**2.61**	1.45%	**2.60**	0.21%	xx	xx	xx	xx	lateral bending	2.25
	2	**4.00**	3.12%	**3.88**	0.73%	**4.34**	2.73%	xx	xx	xx	xx	xx	xx	lateral bending	4.36
	3	**7.31**	1.17%	**7.24**	1.11%	**7.33**	1.87%	**7.28**	0.50%	xx	xx	xx	xx	Vertical bending	7.28
	4	xx	xx	xx	xx	**8.16**	1.03%	8.13	0.54%	xx	xx	xx	xx	Vertical bending	7.87
	5	**8.97**	2.97%	**9.08**	0.59%	**9.09**	1.35%	xx	xx	xx	xx	xx	xx	torsion	8.11
58	1	**12.89**	2.88%	**13.13**	1.12%	**13.06**	2.85%	**13.13**	2.33%	**13.06**	3.06%	**13.11**	3.20%	Vertical bending	12.66
	2	**23.22**	2.05%	xx	xx	**21.50**	2.95%	**21.84**	4.29%	**20.59**	1.83%	**20.71**	0.87%	torsion	23.33

Table 4 Frequency variation considering: a) Method of analysis (SSI x EFDD) and b) Type of records (DWxFV, AVxDW and AVxFV)

Bridge	N	Mode Type	SSSIxEFDD			SSI			EFDD		
			FV	DW	AV	DWxFV	AVxDW	AVxFV	DWxFV	AVxDW	AVxFV
b	1	vertical bending	2.9%	0.2%	0.5%	1.3%	2.2%	3.5%	1.8%	3.0%	1.2%
	2	vertical bending									
	3	vert.&lat. bending	0.2%		0.7%	12.2%	5.2%	7.0%			7.9%
	4	torsion		0.2%		0.6%				1.7%	
15	1	lateral bending			0.4%						
	2	vertical bending			0.1%			0.1%			
	3	lateral bending									
	4	vertical bending									
	5	vertical bending			0.7%			0.4%			
20	1	lateral bending		0.3%		1.2%					
	2	lateral bending	3.2%			8.1%					
	3	vertical bending	1.0%	0.7%		0.3%			0.6%		
	4	vertical bending		0.4%							
	5	torsion	1.2%			1.3%					
58	1	vertical bending	1.8%	0.5%	0.4%	1.3%	0.0%	1.3%	0.0%	0.2%	0.2%5.3%
	2	torsion		1.6%	0.6%	7.7%	4.3%	12.0%			

To investigate the influence of the type of record (free vibration, drop weight and ambient vibration) and the methods of analysis (SSI and EFDD) on the results obtained in this work, the variation between the values of natural frequency identified were calculated and are shown in Table 4. This variation is the difference between two values divided by the average of the two values, shown as a percentage and is given by Eq. (1).

$$Variation(\%) = \frac{|f_i - f_j|}{(f_i + f_j)/2} \times 100 \quad (1)$$

Where f_i and f_j are two corresponding natural frequencies obtained by different methods and excitations sources. It can be noted that the type of record used for analysis affects more the value of the frequency identified than the method used to identify it. As seen in Fig. 6, the average values of frequency variation are less than 2% considering the method of analysis SSI and EFDD. On the other hand, the maximum variation of frequencies identified for each type of records is 12.2% (Table 4) but the mean values are between 2.5% and 4.1% except for one case (Fig. 6). Particularly for this case, which compares frequencies identified in drop weight and free vibration

records using EFDD method, all samples are belonging to well excited first vertical modes of B5, B20 and B58A (Table 4).

Using Eq. (1), it can be seen that variations between numerical and experimental modes can reach up to 14% (Fig. 7) However, if we have the numerical frequencies plot against the average value of all the corresponding experimental frequencies from FV, DW and AV, the data fit to a line of 45 degrees, showing a good agreement between the measured and computed natural frequencies (Fig. 8). The Modal Assurance Criteria (MAC) was applied to check the modal shape configuration agreement between experimental modes and between experimental and numerical modes (Table 5). In general, MAC values between experimental mode shapes are close to 1, except for some cases in B20 and B58A. The comparison with numerical modes shows MAC values also close to 1, except for lateral mode shapes identified in B15 and B20 and on torsional mode shape identified in B20, which is a complex mode.

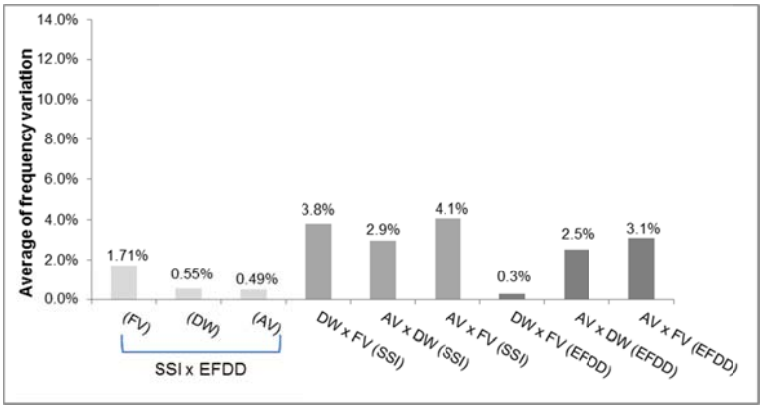

Fig. 6 Average of frequency variation (Method of analysis and Types of records)

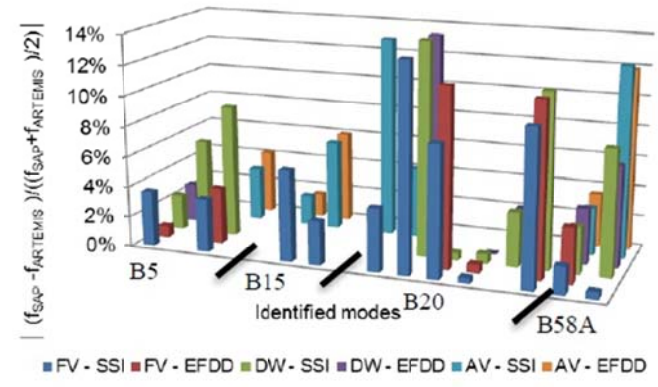

Fig. 7 Matrix of Variation between numerical and experimental frequency values for each type of records and method of analysis for all bridges

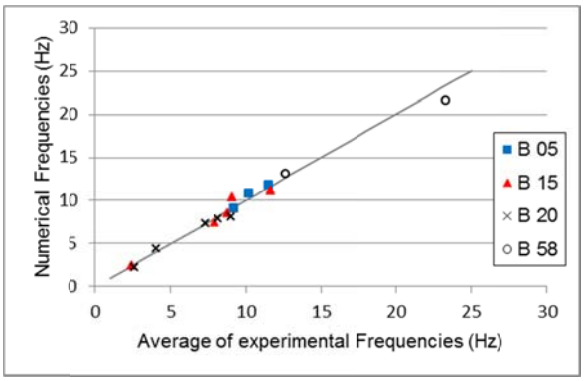

Fig. 8 Numerical Frequencies Vs Average of Experimental frequencies, after the model adjustment

Table 5 Modal Assurance Criteria: Experimental X Experimental mode shapes and Numerical X Experimental mode shapes

Mode Type	MAC between experimental modes	MAC Experimental X Numerical modes
vertical bending	0.85< MAC >0.99	0.94 <MAC >0.98
vertical bending	xx	0.88
vert.&lat. bending	0.78< MAC >0.99	0.72 <MAC >0.83
torsion	0.86< MAC >0.95	xx
lateral bending	0.94	0.48< MAC >0.57
vertical bending	0.95< MAC >0.99	0.61< MAC >0.65
lateral bending	xx	0.60
vertical bending	xx	0.67
vertical bending	0.86< MAC >0.97	0.92< MAC >0.94
lateral bending	0.70< MAC >0.90	0.52< MAC >0.58
lateral bending	0.70< MAC >0.98	0.58< MAC >0.65
vertical bending	0.63< MAC >0.98	0.84< MAC >0.97
vertical bending	0.80	0.71< MAC >0.79
torsion	0.55< MAC >0.78	0.31< MAC >0.54
vertical bending	0.87< MAC >0.99	0.85< MAC >0.97
torsion	0.64< MAC >0.99	0.79< MAC >0.83

6. Finite element models

As part of the research project, finite element models were built for future performance evaluations under current and increased loading conditions. With this main objective in mind and considering the large quantity of models to be built in a limited period of time and also the accuracy of analysis, models in various degrees of refinement were developed for the first set of bridges analysed. It was observed that, except for bridges with very distinct characteristics such as B58A, it would be good enough for our purposes to model the reinforced concrete span as a unique frame element with a pi-shaped section. This choice, however, prevents, in the dynamic analysis, to verify the torsional modes of the bridge deck. So, in this article, as Bridges B20 and

B15 were in the group of the first bridges analyzed and Bridge 58A is very distinct from others, two types of models were developed, one considers the bridge deck as a unique frame element for Bridge B5 and the other model the bridge deck was modeled using shell elements for Bridges B15, B20 and B58A, as shown in Fig. 9. They are better described as follows.

The commercial software SAP 2000 was used to build the FE models. All finite element models were based on the assumptions of linear, isotropic, and homogeneous material behavior. The values of the E-modulus adopted for concrete initially were obtained from various relevant bridge projects. Then, E-modulus of concrete was evaluated from laboratory compression tests on core samples (minimum of two) extracted from various structural elements. These actual material properties were then used to update FE models of bridges (Table 6).

Modal data (natural frequencies and mode shapes) extracted in experimental analysis were used as a target for model parameter adjustment. The parameters modified during the updating were: 1) spring stiffness of end bearing pads; 2) spring stiffness of intermediate bearing pads; 3) E-modulus of bridge deck and 4) E-modulus of Bridge columns. The adjustment was done manually.

6.1 Bridge B5

Bridge B5 was modeled using frame elements for the reinforced concrete spans and caissons; and shell elements for the abutments and caisson caps. The two reinforced concrete I-shaped stringers and the deck slab were modeled as a unique frame element with a pi-shaped section, and Timoshenko's plane-section assumption was adopted. The variation in the web thickness of the stringers was taken into account by using nonprismatic elements. Each span was subdivided into 10 elements to better represent the dynamic behavior of the bridge. The neoprene elastomeric bearings were modeled as SAP2000 link elements. The stiffness of each bearing was calculated according to empirical expressions presented in Pfeil (1989). To precisely represent the soil stiffness, the piles were discretized into 50 frame elements; each about 1 m in length, and a linear spring (link element) with translational stiffness in three directions was attached to each joint. The values of this stiffness were obtained from studies of the soil profile in previously conducted standard penetration tests (SPTs). Additional mass on the deck (due to ballast, sleepers, rails, fastenings, etc.,) was carefully taken into account as linear mass per unit length.

Table 6 Actual E-modulus of concrete evaluated from compression tests on core samples

	E-modulus (MPa)			
Bridge	Deck	Abutment	Column	Caisson cap
B5	48.7	39.3	xx	42.3
B15	24.6	27.2	xx	40.5
B20	26.1	31.5	34.9	xx
B58A	35.7	47.5	xx	xx

6.2 Bridges B15, B20 and B58A

The models of B15, B20 and B58A are almost the same as B5 except for the deck which is modelled using shell elements. Additional mass on the deck (due to ballast, sleepers, rails, fastenings, etc.) was applied as uniform surface mass per unit area. In Bridge B15, solid elements were also used to represent the abutments blocks.

It should be noted that the condition of the beam with clamped end in the abutment, proposed in design for some bridges, as Bridges B15 and B20, is not consistent with the numerical model above., In the nodes corresponding to this supposed clamped section, there are considerable displacements, so the abutment, which should represent a clamped condition, moves with the structure, as observed in the deformed configuration of Fig. 10. This difference on support condition was also confirmed by visual inspections, since cracks of 0.5mm and 1mm were identified at approximately 2/3 of 1st span length. The bending moment diagrams of B15 are shown in Fig. 11 for two types of boundary conditions: a) modelling the abutment and b) with first end clamped. The increasing on tensile forces on lower face of stringer is observed.

For Bridge B15, it can be seen that the natural frequencies are, in general, higher when the end is clamped, except for the fourth lateral bending mode which shows the opposite (Table 7).It happens because as the model configuration is modified and the length between the first two nodes on the mode shape is larger in the case with the clamped end modelling, so the frequency is lower (Fig. 12). Besides, it can be noted that mode 38 of the FEM model with abutment, also identified on experimental analysis, was missed in the FEM model with first end clamped. There is no variation on frequency 7.39 Hz, between the two models, since it is a vertical mode only in the third span, so the boundary condition on first end does not affect it much.

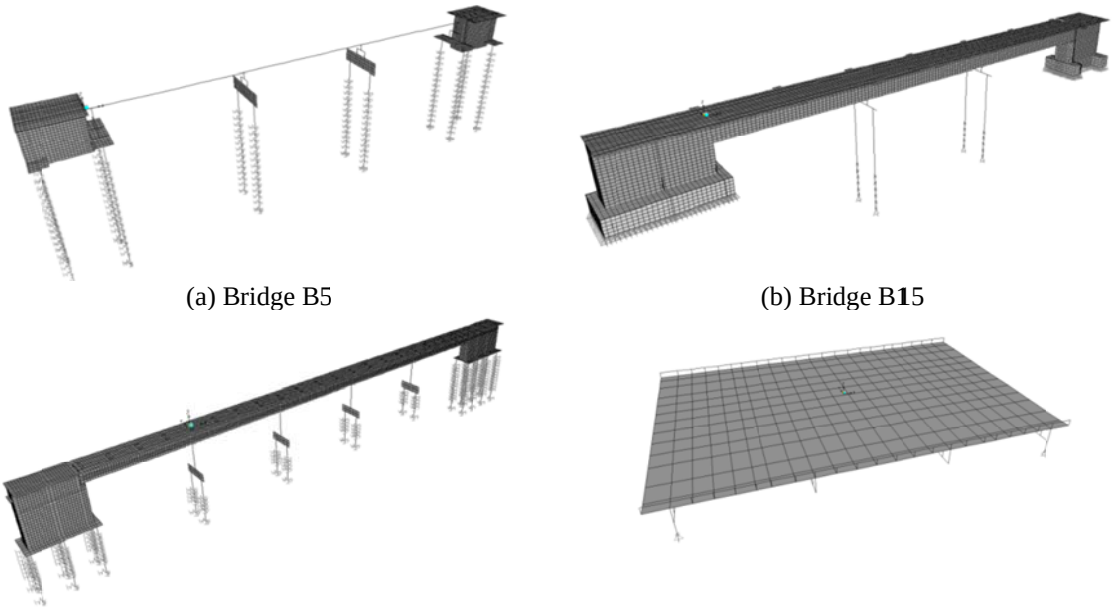

(a) Bridge B5 (b) Bridge B15

(c) Bridge B20 (d) Bridge B58A

Fig. 9 Finite element model of Bridges B5, B15, B20 and B58A

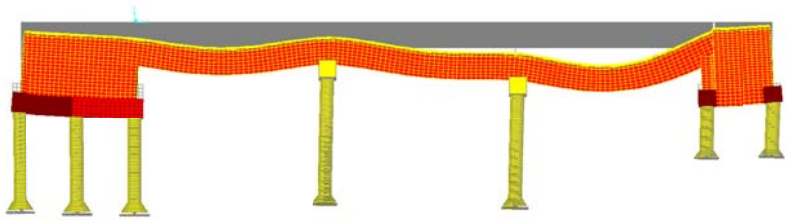

Fig. 10 Side View with deformed configuration, showing motion of abutment. (B15)

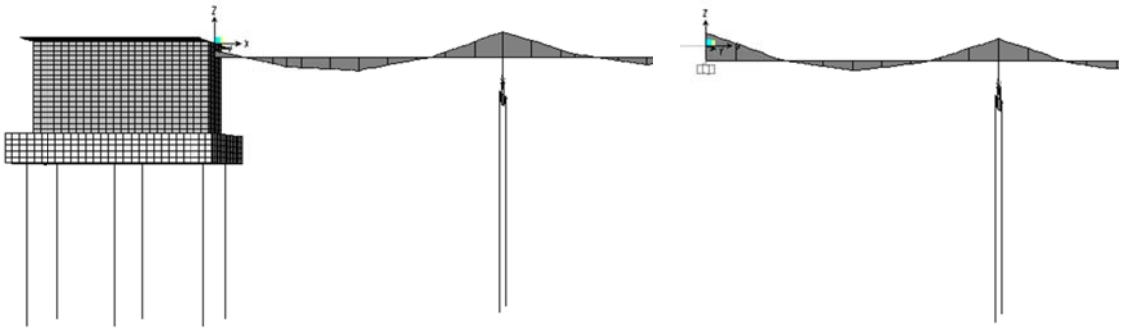

(a) abutment model (b) clamped end

Fig. 11Bending moment diagram for permanent load of 1st span of Bridge B15

Table 7 Natural frequencies of Bridge B15 FE model, considering abutment model and clamped end

Model with Abutment		Model with first end Clamped		Mode Type	Absolute difference
Mode	Freq. (Hz)	Mode	Freq.(Hz)		
1	0.82	1	0.95	Lateral bending	17%
5	2.41	5	2.57	Lateral bending	7%
9	2.63	8	2.72	Lateral bending	3%
22	**7.39**	**18**	**7.39**	**Vertical bending 3rd span**	**0%**
37	**8.78**	**20**	**7.56**	**Lateral bending**	**14%**
24	7.92	21	8.30	Vertical bending	5%
38	**9.11**	**xx**	**xx**	**Vertical bending**	**xx**
44	11.68	28	12.12	Vertical bending 1st span	4%

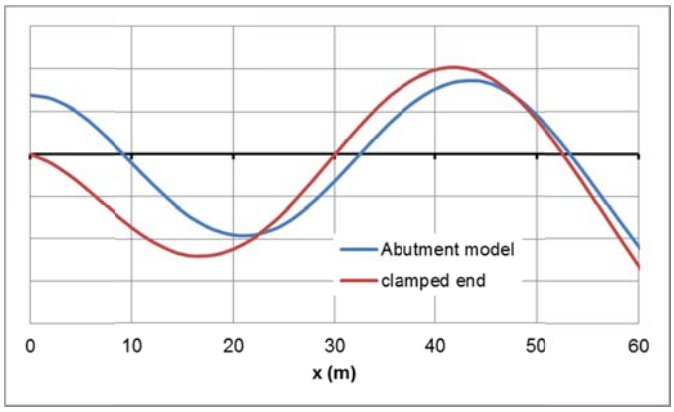

Fig. 12 Mode shape configuration of Bridge B15: mode 37 for model with abutment and mode 20 for model with 1st end clamped

7. Conclusions

Dynamic tests were performed on four bridges, B5, B15, B20 and B58A, crossing the Carajás railway in northern Brazil using three different excitations sources: drop weight, free vibration after train passage, and ambient conditions. To extract the dynamic parameters from the recorded data, Stochastic Subspace Identification and Frequency Domain Decomposition methods were used. Finite-element models were constructed to support and validate the dynamic measurements. Keeping in mind the purposes of this paper are to share experience gained and provide a method to obtain dynamic characteristics, the results show good agreement between the measured and computed natural frequencies and mode shapes. As the model updating was done manually, in the future, a supplementary tuning using recent technique of model updating, which permits to use a higher number of variables, would be desirable, especially if FE model is built with the purpose to better understand the bridge structural behaviour.

Among the techniques used in analysis, the SSI method was the most effective in most cases. In Bridge B15 for free vibration, it was not possible to identify any natural frequency using the EFDD technique, on other hand using SSI technique three frequencies were identified. However, frequency values obtained using both techniques presenting low variations, less than 2%.

The use of projection channels technique and harmonic detection were investigated. Projection channels shown to be an important tool on SSI analysis, but the harmonic detection did not affect significantly the results.

The type of excitation influences on the results more than the technique of analysis. The variation in the values of frequency was found to be significant when types of excitation are compared. Furthermore, in results we can see that drop weight tests were more effective. For bridges B05, B20 and B58A all measured modes were identified in drop weight tests. For ambient vibration and free vibration tests, a similar number of frequencies were identified in each bridge and some frequencies were missed.

However, the choice for which type of excitation is also related with logistic issues. Drop weight tests are difficult to perform, once a drop weight system has to be built and a considerable

time window without traffic is necessary, depending on the number of spans. If the bridge has a high number of spans it becomes unfeasible.

Ambient vibration tests in case of heavy-haul railway bridges also require a considerable time without traffic, since the train–bridge mass relation is high and in this case the system (train-bridge) dynamic properties are different from the bridge dynamic properties. This time window depends on bridge natural period and also on the ambient conditions such as wind velocity. For bridge B58A, according to Table 2, the time length for ambient vibration was 25 min and it was sufficient to identify the first bending frequency of the structure, which was 12.66 Hz in vertical direction. But for Bridge B5, with the same time length of record, only the first vertical frequency (9.24 Hz) was identified and lateral lower bending modes were missed. Finally, for bridge B15, with a record much longer, 59 min, but lower natural frequencies, the lower mode identified was the third lateral bending.

Free vibration tests were performed considering the record obtained after the passage of loaded trains, the amplitude decay time was sufficient for mode identification in these cases.

Based on the testing of 25 number of railway bridges, categorising 4 types, the paper provides guideline on methods of excitation, record length of time, methods of modal analysis including the use of projected channel and harmonic detection. This can help people obtain good dynamic characteristics from measurement data and consequently is useful for model updating to obtain good model for prediction of structural behaviour as well as damage detection.

Acknowledgments

Part of this work was developed in Queensland University of Technology with financial support of CNPQ. The field studies on those bridges presented in this paper was performed by a joint UFPA/VALE research team. The writers gratefully acknowledge the corresponding funding support provided by VALE and also wish to specially acknowledge the following field team members: Vinicius Barichello, Edilson Silva, Jennefer Lavor, Eduardo Tagliarini, Ariany Silva, Carlos Castro and Caio Laurindo for their cooperation and help during the tests. Useful discussions with Prof. Remo Magalhães de Souza (Federal University of Pará) are also acknowledged with thanks.

References

Brincker, R. (2000), “Modal identification from ambient responses using frequency domain decomposition”, *Proceedings of the IMAC-XVIII: Conference on Structural Dynamics*, San Antonio, Texas, USA, February.

Brinker, R., Zhang, L. and Anderson, P. (2001), “Modal identification of output-only systems using frequency domain decomposition”, *Smart Mater. Struct.*, **10**, 441-445.

Herlufsen, H., Andersen, P., Gade, S. and Møller, N. (2006), “Identification techniques for operational modal analysis – an overview and practical experiences”, *Proceedings of the IMAC-XXIV: Conference on Structural Dynamics*, St Louis, Missouri, USA, January.

Jacobsen, N.J., Andersen, P. and Brincker, R. (2007), “Eliminating the influence of harmonic components in operational modal analysis”, *Proceedings of the* IMAC-XXV: *Conference and exposition on Structural Dynamics*, Orlando, Florida, USA, February.

Lee, C.H., Kawatanib, M., Kim, C.W., Nishimura, N. and Kobayashi, Y. (2006), “Dynamic response of a

monorail steel bridge under a moving train", *J. Sound Vib*., **294**, 562-579.
Moradipour, P., Chan T.H.T. and Gallage, C. (2015), "An improved modal strain energy method for structural damage detection, 2D simulation", *Struct. Eng. Mech*., **54**(1), 105-119.
Nguyen, T., Chan, T.H.T. and Thambiratnam, D.P. (2014a), "Effects of wireless sensor network uncertainties on output-only modal analysis employing merged data of multiple tests", *In PLSE special issue – Adv. Struct. Eng*., **17**(3), (in press).
Nguyen, T., Chan, T.H.T. and Thambiratnam, D.P. (2014b), "Effects of wireless sensor network uncertainties on output-only modal-based damage identification", *Aus. J. Struct. Eng.*, **15**(1), 15-25.
Peeters, B. (2000), *System Identification an Damage detection in Civil Engineering*, Ph.D. Thesis, Katholieke Universiteit Leuven, Leuven, Belgium.
Pfeil, W. (1989), *Pontes em Concreto Armado*, LPC Editora, Rio de Janeiro, RJ, Brazil (in Portuguese).
Ren, W.X., Peng, X.L and, Lin, Y.Q.(2005), "Experimental and analytical studies on dynamic characteristics of a large span cable-stayed bridge", *Eng. Struct.*, **27**(4), 535-548.
Shih W.W., Thambiratnam D.P. and Chan T.H.T. (2011), "Damage detection in truss bridges using vibration based multi-criteria approach", *Struct. Eng. Mech*., **39**(2), 187-206.
SVS (2011), *ARTeMIS Extractor release 5.3, User's manual*. Structural Vibration Solutions A/S. <http://www.svibs.com>
Ubertini, F., Gentile, C. and Materazzi, A.L. (2013), "Automated modal identification in operational conditions and its application to bridges", *Eng. Struct*., **46**, 264-278.
Van Overschee, P. and De Moor, B. (1993), "Subspace algorithms for the stochastic identification problem", *Automatica*, **29**(3), 649-660.